



HAL
open science

Study of Intermediate States of Ge-Rich GeSbTe Phase Change Memories by Impedance Spectroscopy

Adrien Delpoux, Sijia Ran, Alain Claverie, Daniel Benoit, Jérémie Grisolia

► **To cite this version:**

Adrien Delpoux, Sijia Ran, Alain Claverie, Daniel Benoit, Jérémie Grisolia. Study of Intermediate States of Ge-Rich GeSbTe Phase Change Memories by Impedance Spectroscopy. 2024 IEEE 5th International Conference on Dielectrics (ICD), Jun 2024, TOULOUSE (FRANCE), France. pp.1-4, 10.1109/ICD59037.2024.10613164 . hal-04780457

HAL Id: hal-04780457

<https://hal.science/hal-04780457v1>

Submitted on 28 Nov 2024

HAL is a multi-disciplinary open access archive for the deposit and dissemination of scientific research documents, whether they are published or not. The documents may come from teaching and research institutions in France or abroad, or from public or private research centers.

L'archive ouverte pluridisciplinaire **HAL**, est destinée au dépôt et à la diffusion de documents scientifiques de niveau recherche, publiés ou non, émanant des établissements d'enseignement et de recherche français ou étrangers, des laboratoires publics ou privés.



Distributed under a Creative Commons Attribution - NonCommercial - ShareAlike 4.0 International License

Study of intermediate states of Ge-rich GeSbTe phase change memories by impedance spectroscopy

Adrien Delpoux¹, Sijia Ran², Alain Claverie², Daniel Benoit³, Jérémie Grisolia^{1*}

¹Laboratoire de Physique & Chimie des Nano-Objets (LPCNO), Toulouse, France

²Centre d'Elaboration de matériaux & d'Etudes Structurales (CEMES-CNRS), Toulouse, France

³STMICROELECTRONICS, Crolles, France

[*jeremie.grisolia@insa-toulouse.fr](mailto:jeremie.grisolia@insa-toulouse.fr)

Abstract— We propose a first investigation of intermediate resistance states of Ge-rich GST (GGST) PCMs by impedance spectroscopy. We highlight that all states present resistive and capacitive components. When switching the memory from the RESET to the SET state the resistance decreases continuously from a low resistance state to a high resistance state while we observe the opposite behavior for the capacitance values. Based on these results, we propose to redefine a state by considering not only the resistance but also the capacitance of the device.

Keywords— GeSbTe alloys, Electrical characterization, Impedance spectroscopy (IS), Phase change memory (PCM), Phase change random access memory (PCRAM), SET, RESET, Intermediate resistance state (IRS).

I. INTRODUCTION

Phase change materials, specifically GeSbTe (GST) alloys, have been largely studied and used for years for their optical properties [1]. More recently, these alloys are of interest to the microelectronics industry due to the possibility to use them as active layers in Phase Change Memories (PCMs) for the next generation of electronics (e.g. neuromorphic electronics, in-memory computing, artificial intelligence...) [2], [3]. A PCM is a component where the active material is a dome of nanometric dimensions that can be switched between a crystalline state and an amorphous state by heating processes. When the dome is crystalline the device has a low resistance (SET state), whereas it has a high resistance when the dome is amorphous (RESET state). This device can be switched from the SET to the RESET state and vice-versa by feeding with adequate electrical pulses causing Joule heating. PCMs are gaining interest due to their fast switching speed ($\sim ns$) [4], [5] and the high contrast of the resistance values defining the memory window ($R_{RESET}/R_{SET} \sim 10^3$) [6]. They also present a high endurance ($\sim 10^{12}$ cycles) and a high scalability [7]. The thermal stability of the amorphous state is a critical parameter of PCMs which often limits the field of applications. To target embedded applications, the crystallization temperature (T_χ) of the chosen alloy must be higher than offered by the canonical $Ge_2Sb_2Te_5$ (GST-225). Ge-rich GST (GGST) alloys [5], [8] provide such thermal stability because they crystallize as a polycrystal made up of grains of several phases [9], [10], all of which are located in or near the dome region of cells programmed in the SET state.

In parallel, discussions about the transport phenomena involved in the PCMs have continued. In literature, the Poole-Frenkel model is mostly used to describe electrical conduction in amorphous GST-225 [11]. However, as put forward in [12], a different transport phenomenon can be

used to describe conduction in GGST alloys, reflecting the strong chemical non-homogeneities possibly found in the amorphous active material. Indeed, Bourguin & al. have shown by extending the conventional study of DC I(V) characteristics to impedance spectroscopy (IS) that the cells show both resistive and capacitive components. They can be represented by RC parallel circuits in both the RESET & SET states and their conduction described using a model commonly used to describe conduction through granular systems [13]. The advantage of IS is the possibility to extract more electrical characteristics (e.g. capacitance or inductance components) than using only classical DC I(V). Thus, this complementary method could help to better understand the electrical conduction in PCMs.

Another interesting possibility demonstrated by PCMs is their ability to show analogical behavior [2], [14]. For this, the resistance is not restricted to the SET and RESET values but can reach any resistance value in between, named Intermediate Resistance States (IRS). In principle, there are two possibilities to access an IRS in a PCM. The access of an IRS from a SET (crystalline) state can be obtained through the partial amorphization of the PCM. Alternatively, the partial crystallization from the RESET state can also lead to an IRS. In some cases, the same IRS can be reached following these two approaches although they may result in significantly different structures and compositions within the cell. The complete analysis of such cells by Transmission Electron Microscopy methods, although efficient, is destructive and very time consuming. This is why complementary characterization by nondestructive and electrical methods is dramatically needed.

The goal of this work is to study PCM cells programmed in RESET, SET, and IRS states using impedance spectroscopy, in addition to traditional DC I(V) measurement. This will allow for a more accurate characterization of the states of the cells by highlighting both their capacitance and resistance.

TABLE I. STATES

State name	Target Resistance	Measured Resistance ($R_s + R$)
SET	20k Ω	24.72k Ω
IRS1	100k Ω	97.66k Ω
IRS2	300k Ω	376.75k Ω
IRS3	500k Ω	565.52k Ω
IRS4	1M Ω	1.19M Ω
IRS5	2M Ω	1.84M Ω
RESET	15M Ω	15.75M Ω

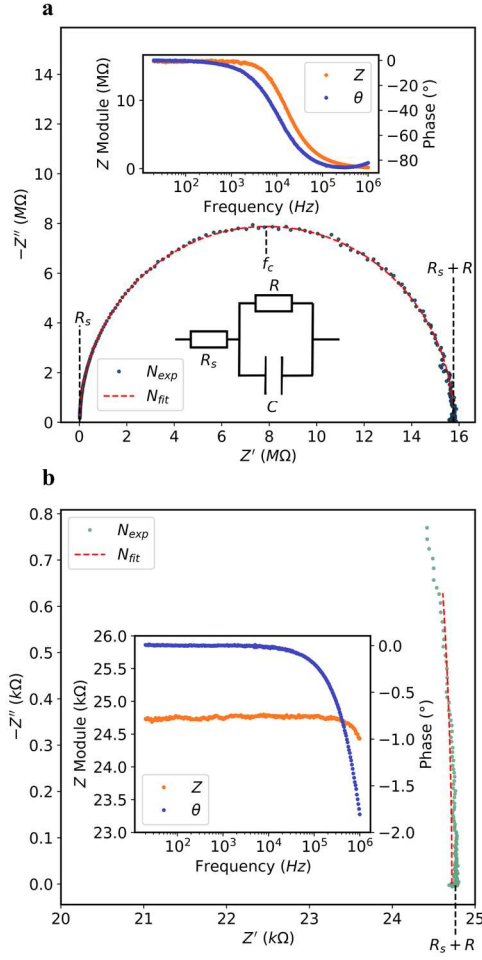


Fig.1. (a), Nyquist plot of the cell in the RESET state. The top inset shows the module (Z) and phase (θ) of the impedance in the RESET state while the equivalent circuit used to fit both curves in the RESET & SET states is shown in the bottom inset. (b), Nyquist plot of the cell in the SET state. The inset shows the evolutions of the module and phase (θ) of this impedance.

II. EXPERIMENTAL SETUP

1. Preparation of samples

a. Design & forming

The PCM devices were fabricated using a wall-shape architecture and contacted via two copper pads connected to the electrodes, as schematically shown in [12]. The PCM is a “1R-type” (1 resistor) and does not include any selector. The device is connected to a probe station JANIS ST-500-1. A Keithley 4200A-SCS equipped with an Ultra-Fast 4225-Pulse Measurement Unit (PMU) and a Source Measurement Unit (SMU) connected to the probe station are used for forming and programming the cells.

The forming process is the first step to perform before programming the memory. From a material point of view, it aims to prepare the cell by amorphizing a dome of a certain volume then re-crystallizing it. This is a critical step as the forming procedure will determine the electrical characteristics and the memory window of the cell. Our forming procedure ensures that the RESET and the SET states are around $15M\Omega$ and $20k\Omega$ respectively and ready to program. After the forming process, 20 RESET/SET cycles are performed to stabilize the cell characteristics.

b. Programming

In order to program the cell in the RESET state, the device is fed by a short ($\sim ns$) and high current electrical pulse (such as $T > T_m$, where T_m is the melting temperature of GST). To reach the SET state, the cell is fed by a longer pulse ($\sim \mu s$) of lower current than used to program the RESET state (such as $T_m > T > T_\chi$) is sent. The IRSs are programmed from the SET state by using partial-RESET pulses (pRESET) of increasing amplitudes to create amorphous domes of increasing sizes, which results in the progressive increase of the resistance of the cells. The pRESET pulses have the same fall time, rise time and width than the RESET pulse except they are of lower amplitudes.

2. Electrical characterization

a. IS measurement

Impedance Spectroscopy (IS) has been carried out using a Keysight E4990A Impedance Analyzer connected to the probe station. The electrical stimulation has a frequency ranging from 20Hz to 1MHz and a peak-to-peak sinusoidal AC amplitude of 100mV, with no DC component. This value is low enough to measure the cells without disturbing them. All measurements (programming and IS) were performed in the dark to avoid any carrier injection into the device. The IS features of each state shown in this article are based on the average of 15 measurements. Every test is run on the same cell, and the 15 measurements, which last approximately 5 minutes, are completed within 3-5 minutes after programming. In addition to the SET and RESET states, 5 IRS have been selected and have been studied in details (cf. Table I). Table I shows the resistances that were targeted and those measured by IS after programming the cells.

b. Fitting procedure

The fitting procedure is based on the electrical equivalent circuit's theoretical impedance, as shown in Fig.1 a. Firstly, R_s is extracted from experimental data from the high frequency measurement (1MHz) and secondly $R_s + R$ is extracted from the low frequency measurement (20Hz). The R resistance is then deduced from the previous measurement. Finally, the fitting algorithm only computes the C capacitance value.

III. RESULTS & DISCUSSION.

1. RESET & SET states

Fig.1a shows the Nyquist plots measured on the cells programmed to the RESET and SET states. The Nyquist plot of the RESET state has a semicircle shape, which shows that the equivalent circuit consists of a resistance R and a capacitance C in parallel. The series resistance R_s mimics the resistance due to the wafer (e.g. heater, interfaces...), the measured resistances reported in Table I represent $R_s + R$. The RESET state demonstrates a substantial modification of the phase above 10 kHz which reaches a value of about -80° at 1MHz whereas the SET state shows only small variations, reaching a value of about $\sim -2^\circ$ at 1MHz. These results are similar to those previously obtained by Bourguine et al. [12]. R_s is extracted from the Nyquist plot

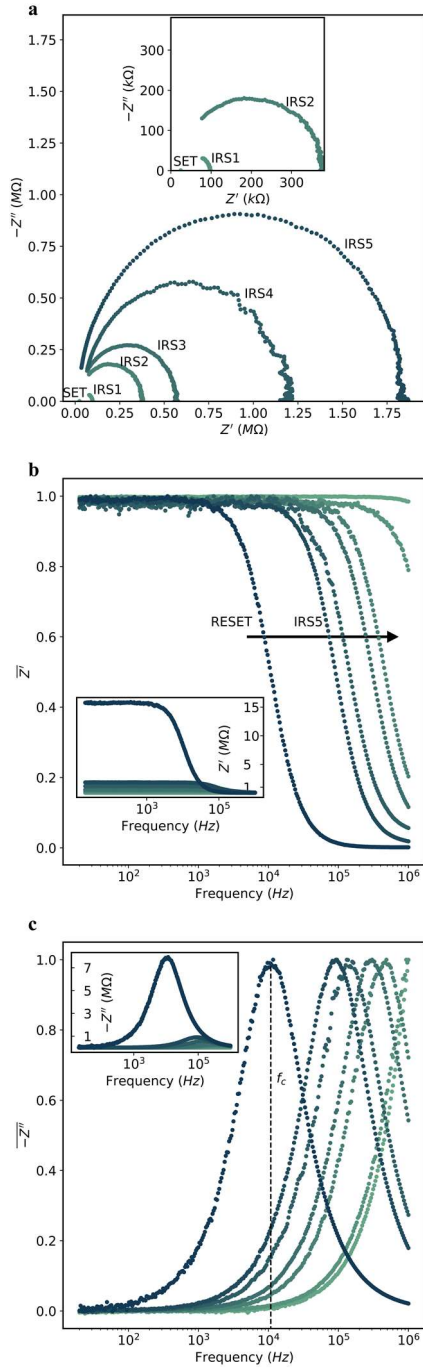


Fig. 2 (a), Nyquist plots of the IRS. The inset is a zoom on the Nyquist plots of the SET state and of IRS1 and IRS2. (b), normalized real parts of the impedance corresponding to each state. The inset shows these real parts before normalization. (c), normalized imaginary parts of the impedance corresponding to each state. The inset shows these imaginary parts before normalization.

characteristic of the RESET state and is about $20k\Omega$ ($\pm 2,5\%$). It will be assumed to be a constant, when analyzing the measurements obtained on the IRS, as all high frequency Nyquist's plots converges to this value (Fig.2 a).

The impedance modulus in the RESET state (inset in Fig.1a) exhibits an abrupt change at around $15kHz$. This sudden transition in the conduction is typical of a RC parallel circuit, when the impedance resulting from the capacitance contribution becomes smaller than the resistance.

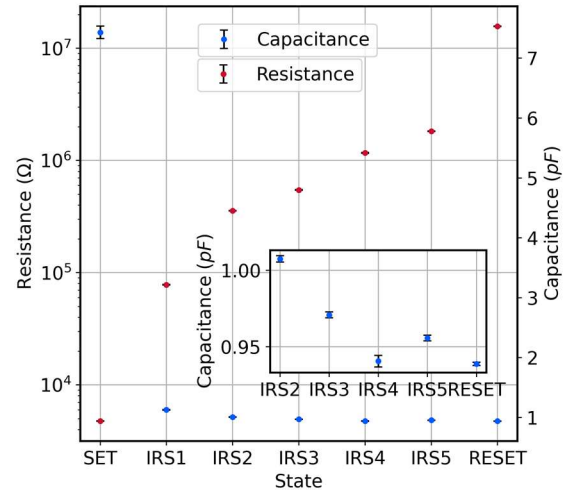


Fig. 3 The value of resistances and capacitances for each state. Capacitance values are obtained by fitting with a maximal error of 2%. Resistances values are extracted from the experimental datas of the inset in Fig. 2b. The maximal error on the measured resistance is 1%.

This is observed at high frequency, and defines the 'capacitive regime' (CR). Alternatively, one can also define a 'resistance regime' (RR), at low frequency. The cutoff frequency f_c ($f_c = 1/2\pi RC$) is the characteristics frequency at which the RR to CR transition occurs. This phenomenon is not observed in the SET state (Fig.1b) as f_c is shifted towards higher frequencies and out of the measurement range of the equipment. Actually, only the onset of this transition is observed, and the Nyquist plot shows only the beginning of a semicircle.

One could think, looking quickly at Fig.1a-b, that the capacitance is larger in the RESET state than in the SET state (high phase and module changes). Actually, the precise measure and fit of the plot gives $R = 15.73 M\Omega$ and $C = 0.94 fF$ for the RESET state and $R = 4.72k\Omega$ and $C = 7.45pF$ for the SET state. The capacitance is thus almost ten times larger in the SET than in the RESET state. This results from the fact that the resistance is divided by almost one thousand when switching from RESET to SET. Interestingly, Huang et al. [15] demonstrated, on GST-based PCM cells, a similar significant capacitance reduction between the SET and RESET states. The cut-off frequency associated to the SET state is calculated to be of about $f_c = 5.74MHz$, the reason for which the transition from RR to CR is observed at much higher frequencies in the SET state.

These results show how closely resistance and capacitance is linked to the material. Indeed, the polycrystalline GGST dome (*i.e.* SET state) is characterized by a low resistance and an important capacitance. According to Huang et al. [15], the high capacitance in the SET state is mostly owing to the presence of grain boundaries in the polycrystalline state. Whereas, the fully amorphous GGST dome (*i.e.* RESET state) shows a high resistance but a low capacitance. Finally, these material characteristics evidence that it is essential to measure both the capacitance and the resistance to fully characterize a state in PCMs.

2. Intermediate resistance states

Fig.2a depicts the IRS Nyquist plots characteristic which exhibit semicircular shapes. As we shift from the IRS5 to the SET state, the semi-circle becomes less and less visible.

The IRS1 and the SET state only show the beginning of the semicircle as f_c is being shifted to high frequencies. To better depict the associated shift frequency, Fig. 2b-c represent the normalization of the real and imaginary parts of the impedance \overline{Z}' and $-\overline{Z}''$, respectively. In these figures, the shift of f_c is clearly visible and continuously increases from the RESET to the SET state. In Fig. 2b, we note that the RR to CR transition is also not occurring for IRS1 within the studied frequency range.

In the hypothesis of R_s constant, Fig.3 illustrates the values of R and C as a function of the programmed states, extracted using the electrical equivalent circuit for the RESET and SET states described in Section 2. When progressing from the SET to RESET state via IRS states, Fig.3 reveals that, the resistance continuously increases while the capacitance continuously decreases. Thus, resistance and capacitance seem to vary in the opposite way. Moreover, Fig.3 shows that the capacitance of IRS monotonously evolves between its maximal and minimal values, obtained for the RESET and SET states, such as $R_{RESET} > R_{IRS} > R_{SET}$ and $C_{SET} \geq C_{IRS} \geq C_{RESET}$. Moreover, the capacitance suddenly decreases from the SET state to IRS2 while is almost constant from IRS4 to the RESET state.

On one hand, the capacitance from the SET state to IRS3 is decreasing. According to the RESET & SET state results, it is a characteristic of a polycrystalline dome with an increasing amorphous size. However, it cannot be ruled out that the high capacitance found in the SET condition may also be due to a non-negligible contribution from amorphous zone residues in these programmed cells [16]. On the other hand, from IRS4 to the RESET state the capacitance is almost constant. These states could be IRSs where the distribution between amorphous and polycrystalline GGST is dominated by the amorphous structure, changing the capacitance to its lower value. As a result, the remaining polycrystalline structures are likely to have a small contribution. This impedance spectroscopy study shows that, beyond the SET and RESET states, the intermediate states must be represented using a couple of parameters (R , C), which vary monotonically in opposite directions and with greater fluctuation around the SET state (i.e. IRS1-2).

IV. CONCLUSION

We propose a first investigation on various intermediate states of Ge-rich GST (GGST) PCMs by impedance spectroscopy. We highlight an important variation of resistance but also capacitance between the SET and RESET states. Moreover, we found a monotonous variation of R and C through SET, IRSs and RESET, that confirm the importance to describe a state with the parameters (R , C). This study demonstrates that the term IRS is overly limited and should be expanded to include the concept of intermediate resistance and capacitance states (IRCS). Moreover, it shows the importance of IS on PCM cells to better understand their electronics properties using a non-destructive method of characterization. However, more research, including comprehensive characterization of the cells using advanced TEM methods [9], is required to confirm the relationship between the electrical properties and the composition (amorphous/crystalline) of the cells. In connection to this, it will then be possible to extract more

electronic properties from these IS results, such as carrier mobilities, as suggested in [17].

ACKNOWLEDGMENT

This research was funded, in whole or in part, by l'Agence Nationale de la Recherche (ANR), project INTERSTATE ANR-22-CE24-0024.

REFERENCES

- [1] N. Yamada, E. Ohno, N. Akahira, K. Nishiuchi, K. Nagata, and M. Takao, 'High Speed Overwritable Phase Change Optical Disk Material', Japanese Journal of Applied Physics, vol. 26, no. S4, p. 61, Jan. 1987.
- [2] M. Le Gallo and A. Sebastian, 'An overview of phase-change memory device physics', Journal of Physics D: Applied Physics, vol. 53, no. 21, p. 213002, Mar. 2020.
- [3] D. V. Christensen et al., '2022 roadmap on neuromorphic computing and engineering', Neuromorphic Computing and Engineering, vol. 2, no. 2, p. 022501, May 2022.
- [4] G. Bruns et al., 'Nanosecond switching in GeTe phase change memory cells', Applied Physics Letters, vol. 95, no. 4, Jul. 2009.
- [5] V. Sousa and G. Navarro, 'Material Engineering for PCM Device Optimization', in Phase Change Memory, Springer International Publishing, 2017, pp. 181–222.
- [6] R. Berthier, N. Bernier, D. Cooper, C. Sabbione, F. Hippert, and P. Noé, 'In situ observation of the impact of surface oxidation on the crystallization mechanism of GeTe phase-change thin films by scanning transmission electron microscopy', Journal of Applied Physics, vol. 122, no. 11, Sep. 2017.
- [7] G. W. Burr et al., 'Phase change memory technology', Journal of Vacuum Science & Technology B, Nanotechnology and Microelectronics: Materials, Processing, Measurement, and Phenomena, vol. 28, no. 2, pp. 223–262, Mar. 2010.
- [8] P. Zuliani et al., 'Overcoming Temperature Limitations in Phase Change Memories With Optimized GexSbyTez', IEEE Transactions on Electron Devices, vol. 60, no. 12, pp. 4020–4026, Dec. 2013.
- [9] M. A. Luong et al., 'On Some Unique Specificities of Ge-Rich GeSbTe Phase-Change Memory Alloys for Nonvolatile Embedded-Memory Applications', physica status solidi (RRL) – Rapid Research Letters, vol. 15, no. 3, Dec. 2020.
- [10] E. Rahier et al., 'Crystallization of Ge-Rich GeSbTe Alloys: The Riddle is Solved', ACS Applied Electronic Materials, vol. 4, no. 6, pp. 2682–2688, May 2022.
- [11] D. Ielmini, 'Electrical Transport in Crystalline and Amorphous Chalcogenide', in Phase Change Memory, Springer International Publishing, 2017, pp. 11–39.
- [12] A. Bourguin et al., 'On the charge transport mechanisms in Ge-rich GeSbTe alloys', Solid-State Electronics, vol. 172, p. 107871, Oct. 2020.
- [13] L. Merle, A. Mlayah, and J. Grisolia, 'Plasmo-electronic properties of self-assembled gold nanoparticles: impedance spectroscopy experiments combined with numerical simulations', Materials Today Nano, vol. 22, p. 100332, Jun. 2023.
- [14] J. Zhu, T. Zhang, Y. Yang, and R. Huang, 'A comprehensive review on emerging artificial neuromorphic devices', Applied Physics Reviews, vol. 7, no. 1, Feb. 2020.
- [15] Y.-H. Huang, Y.-J. Huang, and T.-E. Hsieh, 'A study of phase transition behaviors of chalcogenide layers using in situ alternative-current impedance spectroscopy', Journal of Applied Physics, vol. 111, no. 12, Jun. 2012.
- [16] L. Laurin et al., 'Unveiling Retention Physical Mechanism of Ge-rich GST ePCM Technology', in 2023 IEEE International Reliability Physics Symposium (IRPS), 2023.
- [17] P. Višćor and M. Višćor, 'Electrical Impedance Spectroscopy: "First Principles" analysis and simulations of electrical response in the classical range of frequencies below 1 THz and the resulting new role of Electrical Impedance Spectroscopy in electrical characterisation within Condensed Matter Physics', Pure and Applied Chemistry, vol. 91, no. 11, pp. 1837–1856, Oct. 2019.